NMR Characterization of Low Hard Segment Thermoplastic Polyurethane/Carbon Nanofiber Composites

Daniel S. Powers,[†] Richard A. Vaia,[†] Hilmar Koerner,[‡] Jennifer Serres,[§] and Peter A. Mirau*,[†]

Air Force Research Laboratory (AFRL/RXBP), Wright-Patterson Air Force Base, Ohio 45433, USA, Universal Technology Corporation, Dayton Ohio 45433, USA, Wright State University, Dayton Ohio 45431, USA

Received February 1, 2008; Revised Manuscript Received April 15, 2008

ABSTRACT: Solid-state proton nuclear magnetic resonance (NMR) has been used to investigate the structure and dynamics of a thermoplastic polyurethane elastomer (TPE) filled with carbon nanofibers (CNF's) for shape-memory applications. The TPE soft segments are above their glass transition temperature (T_g) at ambient temperature and give rise to relatively narrow (∼2 kHz) signals in the solid-state proton spectrum. The introduction of CNF's leads to a concentration-dependent shifting and broadening of the signals, while the proton spin−lattice and spin−spin relaxation times are not significantly altered, showing that the broadening is inhomogeneous and related to the difference in magnetic susceptibility between the TPE and the CNF's. Proton spin diffusion experiments reveal the onset of stress-induced crystallinity as the samples are stretched to 60%, and stretching to 1000% leads to crystallization at the CNF surface and increased separation between the CNF's and the mobile amorphous phase of the TPE. The implications for the mixing of polymers and CNF's are considered.

Introduction

Shape memory polymers (SMP's) have the unique ability to "remember" their original shape after some deformation and are of interest as actuators and sensors.[1] Conventional processing techniques are used to provide the "parent" shape, while the application of external stimuli, such as stretching above T_g or the crystallization temperature, give rise to a new temporary shape. SMP's are actuated and return to their original shape following the application of a second external stimulus. A number of polymers have excellent shape−memory properties, including polyethers, polyacrylates, polyurethanes, epoxies, polyamides, polynorbornenes, styrene−butadiene copolymers, polyisoprene, and cross-linked polyethylene.[2,3] The most widely used SMP's are urethane-based thermoplastic elastomers (TPE's).

Thermoplastic polyurethane elastomers have many desirable properties including high elongation to break, high strength, good abrasion resistance, a high elastic modulus compared to other elastomers,[4] and they are frequently used in aerospace, automotive, electronics, and petrochemical applications. Polyurethanes are considered linear segmented block copolymers because they are made up of alternating sequences of "hard" and "soft" segments that phase separate into domains.[5] The hard segments are typically composed of diisocyanate chain extenders, while the soft segments contain flexible polyether or polyester diol chains.[6] These long flexible chains connect the hard segments and give the polymer its elastomeric properties, and during tensile deformation these soft segments uncoil and allow the polymer to stretch several times its original length. It is the entropic energy stored in these soft segments that provides the driving energy to return the polymer to its original shape, while the hard segments behave as pinning points that "remember" the original shape. It is apparent from a review of the literature that most polyurethanes contain a large fraction of hard segments (∼40−50%).[7] The TPE used in this study (Irogran) contains a much lower fraction of hard segments (<10%), and the hard segments are physically rather than chemically cross-linked. The resulting material exhibits lower recoverability following elongation than most cross-linked elastomers.

Carbon nanofibers (CNF's) are a new class of polymer filler material with unique structures, as well as excellent mechanical and electrical properties.[8] Within the past decade carbon nanotubes (CNT's) and CNF's (heat-treated multiwall CNT's) have been evaluated as reinforcing agents because of their high aspect ratios, which lead to property improvements at much lower weight fractions (0.5−5%) than required for conventional fillers (30−50%).[9] The lower loadings decrease the solution viscosity, allowing for easier processing. As with conventional fillers, good dispersions and strong interfacial interactions are important for the property improvements. We have used CNF's in these studies because they are orders of magnitude less expensive than single- or multiwalled CNT's.

Nuclear magnetic resonance (NMR) is a powerful method to study the structure and dynamics of complex and heterogeneous systems because the spectroscopy properties (chemical shifts, relaxation times, and line widths) depend on the local structure and dynamics.[10] Advanced NMR methods have been especially successful in characterizing the structure and dynamics of TPE's.[11−14] The challenge in understanding nanocomposites is to isolate the signal from the interfaces so that the structure and dynamics of interfacial materials can be studied. NMR methods have been successfully applied to interfaces in clay,[15−17] silica,[18,19] and other composites, but the study of CNT's and CNF's has proven more challenging. This is due in part to the synthetic methods that produce mixtures of tube types and the presence of residual paramagnetic catalysts.[8] Theoretical studies have shown that the carbon chemical shift and magnetic susceptibility for single-walled CNT's depends on the tube type (metallic or semiconducting), the structure, and the diameter.[20] We would expect these property variations to be even larger for multiwalled nanotubes or CNF's, as they are intrinsically more heterogeneous materials. The TPE/CNF composites have improved the shape−memory properties relative to the TPE,

* Corresponding author. Telephone: +1937 255 8979. Fax: +1937 255 9157. E-mail address: peter.mirau@wpafb.af.mil.
[†] Air Force Research Laboratory (AFRL/RXBP), Wright-Patterson Air Force Base.
[‡] Universal Technology Corporation.
[§] Wright State University.

10.1021/ma8002483 CCC: $40.75
Published on Web 05/30/2008

Scheme 1. Structure and Proton Assignments for Irogran

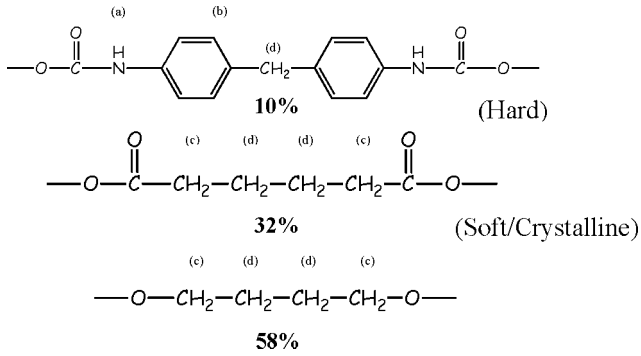

and the electrical and thermal properties of the CNF's provide additional mechanisms for actuation.[9]

Our initial solid-state carbon NMR studies using cross polarization and magic-angle sample spinning of the CNF/TPE composites showed that it is difficult to directly observe the CNF's or polymer chains in close proximity to the CNF's (not shown). These data suggest that signals in the vicinity of CNF's are absent from the spectra either due to a distribution in magnetic susceptibilities resulting from wide structural variations in the CNF's or from residual paramagnetic catalysts that broaden the NMR signals. To investigate the structure and dynamics of the CNF/TPE composites we have used the proton signals from the mobile fraction of the thermoplastic elastomer as an indirect measure of the interfacial structure. The mobile fraction is far above the polymer T_g at ambient temperature and can be directly observed in films with a good signal-to-noise ratio using a high-resolution proton NMR probe. Using this approach we are able to monitor the proximity of the CNF's to the mobile fraction, the effect of CNF's on the polymer dynamics, and the domain sizes for the rigid and mobile segments as a function of CNF concentration and external stress.

Methods and Materials

Materials. Irogran PS455−203 (formerly called Morthane) (Scheme 1) is a high performance thermoplastic polyurethane elastomer purchased from Huntsman Polyurethane. NMR analysis in $CDCl_3$ shows that Irogran contains ∼10% aromatic diisocyanate (hard segment), ∼32% aliphatic and cyclo-aliphatic dicarboxylic acids and ∼58% aliphatic diols (soft segments).[9] Irogran has a density of 1.19 g/cm,[3] and DSC studies show a T_g at −45 °C that can be assigned to the mobile amorphous phase. The melting temperature (T_m) for the soft-segment crystallites is 48 °C.

The CNF's used in these studies were heat-treated vapor-grown carbon nanofibers (PR-19-HHT) from Applied Science Incorporated with a density of 2.1 g/cm^3. The average diameters and lengths of the CNF's were 100 nm and greater than 10 μm, as measured by a scanning electron microscopy. Chemical analysis shows that PR-19-HHT contains 99.9% carbon with hydrogen, nitrogen and iron levels below 0.1%, 0.1% and 0.024%, respectively.

Polymer Nanocomposite Fabrication. The Irogran/CNF composites were prepared using a solution mixing process.[21] Solid pellets of Irogran were dissolved in tetrahydrofuran (THF) at ambient temperature (∼25 °C) for 4 h with magnetic stirring. A CNF/THF mixture was prepared in a separate reaction vessel under shear for 4 h using an Ultra Turrax IKA T18 Basic Stirring Machine operating at 14 000 rpm. This shearing process was used to break up any large clumps and evenly disperse the CNF's in the THF. Once evenly dispersed, the CNF/THF mixture was poured into the Irogran/THF mixture and allowed to mix for 24 h to maximize dispersion of the nanofibers in the polymer matrix. The stirring container was open to the atmosphere and the majority of the THF solvent evaporated during this period. The remaining relatively viscous solution was poured into Teflon molds (102 mm × 26 mm), covered with aluminum foil and allowed to air-dry overnight. The specimens were removed from the molds and placed in a vacuum oven for 24 h at 45 °C to remove any excess THF. The dried composite samples were then stored in a desiccator at room temperature prior to measurement.

Deformation and Setting. The films for NMR experiments were as-cast samples ($\lambda = 1.0$) or samples stretched to 60% ($\lambda = 1.6$) or 1000% ($\lambda = 11$). Samples at 60% strain were prepared using a TA Instruments dynamic mechanical analyzer (DMA Model 2980). Microtensile specimens (8 mm (length) × 4 mm (width) × 0.5 mm (thickness)) were cut from sheets formed in the Teflon molds and placed in the DMA. The samples were stretched at 0.2 N/min to 60% strain at ambient temperature (25 °C). After 30 min, the strain was removed and the sample was allowed to partially relax, and this partially relaxed sample was used for NMR experiments. For the larger strain experiments, microtensile samples of the same size were placed in a Tinius Olsen Universal Testing Machine (Model H10K-S UTM) and the samples were strained to 1000% at a rate of 2 mm/min at ambient temperature.

Solid State Proton NMR Experiments. Solid-state proton NMR spectra were acquired at 500 MHz using a Tecmag Apollo NMR spectrometer. Small samples of the films (1 mm × 5 mm) were placed in 4 mm NMR tubes that were inserted into 5 mm NMR tubes for acquisition of the proton NMR spectra using a high-resolution NMR probe. The spectra were acquired with a sweep width of 20 kHz using a 12 μs 90° pulse. The chemical shifts were referenced to a lightly cross-linked sample of poly(dimethyl siloxane) at 0 ppm. The spectra of the samples were recorded in the same NMR tube directly after acquisition of the reference samples to account for any differences in magnetic susceptibilities of the NMR tubes. The proton spin−lattice (T_1) and spin−spin (T_2) relaxation times were measured using the inversion−recovery and Carr-Purcell Gill-Meiboom pulse sequences.[22] Both the T_1 and T_2 relaxation times were adequately fit with a single-exponential function and no differences in relaxation times were observed for different parts of the proton line. We estimate that the uncertainties in the relaxation times are on the order of 10%. The domain sizes were measured by spin diffusion using the Goldman−Shen pulse sequence[23] with a delay time (τ_0) of 50 μs to create a polarization gradient. The spin diffusion curves were corrected for T_1 relaxation.[24]

Results and Discussion

The TPE/CNF composites are complex materials containing phase-separated polymer hard segments, amorphous soft segments above T_g, crystalline dicarboxylic acid and diol segments and CNF's. The morphology has been reported to change significantly as a function of temperature and external stress.[9,25] We have studied these materials using solid-state proton NMR since our initial carbon NMR studies showed a low signal-to-noise ratio (not shown) for the polymer chains in close proximity to the CNF's. Proton NMR is not typically used to study the structure and dynamics of solid polymers because the line widths are much larger than the chemical shift dispersion for polymers below their glass transition temperatures. However, above T_g or with fast magic-angle sample spinning, relatively high resolution spectra can be obtained.[10,26,27] The proton NMR spectra, line widths, and relaxation times are sensitive to the molecular dynamics and the presence of paramagnetic atoms.

Figure 1 compares the 500 MHz proton NMR spectra of the TPE dissolved in THF-d_8 and the as-cast film. The solution spectrum shows very narrow lines and a chemical shift dispersion from the different chemical groups shown in Scheme 1. The proton spectrum of the film is not well resolved and shows a single broad peak with a full-width at half-maximum of ∼2 kHz. We assign this signal to the mobile amorphous phase, since the peaks from crystalline soft segments and the aromatic hard segments are too broad to observe using high-resolution NMR. In the following experiments we use the signals from the mobile

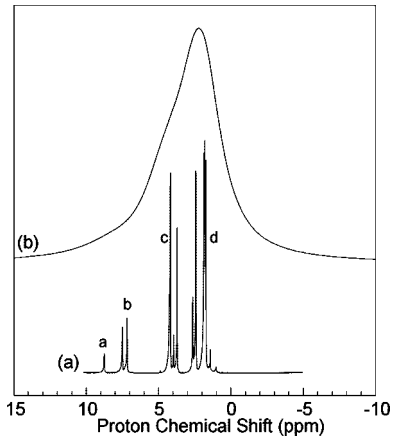

Figure 1. 500 MHz proton NMR spectra of (a) Irogran dissolved in THF-d_8 and (b) the as-cast film (see Scheme 1 for proton assignments).

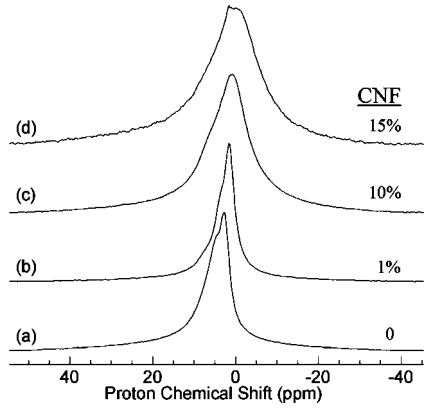

Figure 2. Proton NMR spectra of as-cast (a) Irogran and composites with (b) 1 wt % CNF, (c) 10 wt % CNF, and (d) 15 wt % CNF.

Table 1. Effect of CNF's on the Proton Chemical Shift (δ_H) and Line Widths ($\Delta\upsilon_{1/2}$) for Irogran Composites

wt % CNF	δ_H (ppm)	$\Delta\upsilon_{1/2}$ (Hz)
0	2.1	1900
1	0.7	2100
10	0.1	5200
15	−1.8	5900

amorphous phase to indirectly measure the structure and dynamics of the polymer chains in close proximity to the CNF's.

Figure 2 shows the 500 MHz proton spectra of as-cast Irogran films containing 0, 1, 10, and 15 wt % CNF's. The addition of nanofibers leads to a concentration-dependent broadening and shifting of the mobile amorphous phase peak (Table 1). The change in chemical shift could be attributed to ring current shifts from CNF's in close proximity to the soft segments or to magnetic susceptibility variations in the composites. The change in line width ($\Delta\upsilon_{1/2}$) could be attributed either to a slowing of chain motion or magnetic susceptibility variations introduced with the CNF's. We can distinguish between these possibilities using relaxation experiments.

Figure 3 shows the effect of stretching on the proton NMR spectra of the mobile amorphous phase for TPE and the 10 wt % CNF composite. Stretching to 60% (the onset point for stress-induced crystallinity) leads to only minor changes in the spectra of both the TPE and the composite, while a much larger stretching (1000%) leads to large downfield chemical shift changes for both samples, and additional line broadening for the TPE film. In contrast to the concentration-dependent shifting and broadening of the signal for the unstretched samples, nearly identical chemical shifts are observed for the samples with and without CNF's. We conclude from this observation that the local magnetic environment for the amorphous chains is similar in both samples, demonstrating that these chains are no longer in close proximity to the CNF's.

The large change in line widths that accompany the addition of CNF's or stretching to 1000% could arise either from homogeneous or inhomogeneous line broadening. Homogeneous broadening occurs when the proton spin−spin relaxation time (T_2) decreases as the molecular dynamics are restricted,[28] and the relationship between the T_2 and the line width is given by:

$$\Delta\upsilon_{1/2} = \frac{1}{\pi T_2} \tag{1}$$

The most likely mechanisms for spin−lattice (T_1) and spin−spin relaxation in these samples are dipolar and paramagnetic interactions.[22,24] These contributions add to the relaxation rate and are given by

$$\frac{1}{T_{1,2}} = \frac{1}{T_{1,2}^{D}} + \frac{1}{T_{1,2}^{P}} + \frac{1}{T_{1,2}^{other}} \tag{2}$$

where $1/T_{1,2}^{D}$, $1/T_{1,2}^{P}$, and $1/T_{1,2}^{other}$ denote the contributions from dipolar, paramagnetic and other possible mechanisms that contribute to the T_1 or T_2 relaxation rates. The point to note for these discussions is that if paramagnetic interactions contribute to the relaxation, they will contribute both to T_1 and T_2 relaxation.

In order to study the sources of relaxation and determine the relative contributions of homogeneous and inhomogeneous line broadening to the line widths, we have measured the T_1 and T_2 relaxation times as a function of CNF concentration and stretching. These relaxation times, along with the homogeneous line widths calculated from the T_2's ($\Delta\upsilon_{1/2}^{calc}$) are compiled in Table 2.

The T_1's are usually not used to study the dynamics of polymers because magnetization can be efficiently transferred between protons at a rate faster than the spin−lattice rate, so the proton T_1's are an average for the entire spin system. However, the presence of paramagnetics provides another relaxation pathway that can significantly decrease the polymer T_1's in nanocomposites.[17] The T_1's for the stretched and as-cast Irogran films and the nanocomposites are in the range of 0.8 to 1.4 s. Since the T_1's do not significantly decrease with the addition of CNF's, these data demonstrate that paramagnetic impurities do not make a significant contribution to the proton relaxation, and that the broader lines observed for the CNF composites are not an artifact of residual catalyst used in the synthesis of the CNF's. These data are consistent with the low iron levels (<0.024%) measured by elemental analysis in the purified CNF's.

The T_2's (Table 2) do not follow any clear trend with respect to stretching or the presence of CNF's. The T_2's for TPE increase as the films are slightly stretched ($\lambda = 1.6$) but then decrease with extreme stretching ($\lambda = 11.0$). The increase in relaxation time with slight stretching is somewhat unexpected, since the stretched films are under stress and we would expect the chains on average to have reduced dynamics and shorter T_2's.[17] Since the T_2's are not greatly affected by the addition of CNF's, we conclude that they do not greatly affect the dynamics of the mobile amorphous phase.

The homogeneous line widths can be calculated from the T_2's using eq 1, and they are listed in Table 2. These data show that the observed line widths are much larger than the values calculated from the T_2's. The chemical shift dispersion (illustrated by the solution spectrum shown in Figure 1a) from the different chemical environments along the chain (aromatic,

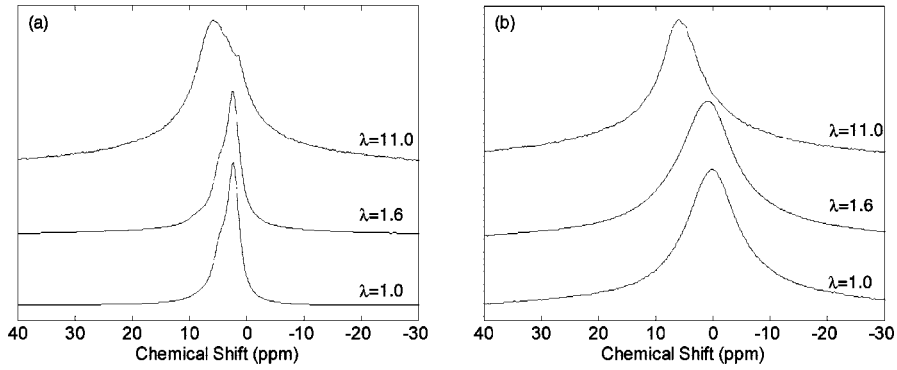

Figure 3. Comparison of the NMR spectra for the stretched and as-cast films (a) without and (b) with 10 wt % CNF.

Table 2. Spin−Lattice Relaxation Times (T_1), Spin−Spin Relaxation Times (T_2), Chemical Shifts (δ_H), and Line Widths (Observed and Calculated) for As-Cast and Stretched Irogran and the 10 wt % CNF Composite

	Irogran			Irogran + 10 wt % CNF		
parameter	$\lambda = 1.0$	$\lambda = 1.6$	$\lambda = 11$	$\lambda = 1.0$	$\lambda = 1.6$	$\lambda = 11$
T_1 (s)	0.82	0.85	1.1	0.89	0.86	1.4
T_2 (ms)	0.40	0.80	0.17	0.30	0.56	0.25
δ_H (ppm)	0.9	1.2	5.9	0.1	0.7	5.9
$\Delta\upsilon_{1/2}^{obs}$ (Hz)	1650	1950	6100	5200	5700	6150
$\Delta\upsilon_{1/2}^{calc}$ (Hz)	796	398	1873	1061	568	1273

aliphatic, etc.) partially explains the broad lines in the films, but it does not explain the broader lines for the CNF composites.

X-ray scattering has shown that the TPE and CNF composites are phase separated into crystalline and amorphous domains, and several transitions, including the soft segment T_g at −45 °C and melting transition at 48 °C, are observed by DSC.[25] We have investigated the morphology in stretched and as-cast films using spin diffusion methods to characterize the mobile and rigid domains sizes. There are a number of pulse sequences that can be used to investigate the domain structure, including the three-pulse Goldman−Shen sequence used in these studies.[23] The spin diffusion pulse sequence creates a polarization gradient between the mobile and rigid phases, and we can calculate the domain sizes by monitoring the rate of magnetization exchange between them.[17,29] Figure 4 shows a plot of the mobile phase peak intensity as a function of spin diffusion time after creation of the polarization gradient for TPE and the 10 wt % composite in the as-cast and slightly stretched ($\lambda = 1.6$) films. The feature to note about Figure 4 is that the spin diffusion data is sensitive to slight stretching and the onset of stress-induced crystallinity. In comparison, changes in the X-ray scattering are not observed until much higher stretching.[25]

Proton spin diffusion has been extensively used to study the morphology of polymers because the rates of spin diffusion are sensitive to domain sizes on the order of 1−20 nm that are difficult to study by other means. The length scale of spin diffusion (L) is related to the shortest diffusion path in a given morphology (lamellar, cylindrical, or spherical). It depends on the surface-to-volume ratio and for a two-phase model is given by[30]

$$L = \frac{4\sqrt{t_{SD}}\sqrt{D_A D_B}(\rho_A^H f_A + \rho_B^H f_B)}{f_A f_B \sqrt{\pi}(\rho_A^H \sqrt{D_A} + \rho_B^H \sqrt{D_B})} \quad (3)$$

where D_A and D_B are the spin diffusion coefficients for the mobile and immobile phases, ρ_A^H and ρ_B^H are the proton densities, f_A and f_B are the volume fractions, and $\sqrt{t_{SD}}$ is measured experimentally. Based purely on geometrical arguments this length scale is converted into the domain size (d) and the long period (d_{lp}), or the distance between domains, for a given morphological model (1D, 2D or 3D).[30,31] The experimental value for the characteristic spin diffusion time, $\sqrt{t_{SD}}$, can be determined from the initial rate of spin diffusion, as shown in Figure 5 for the as-cast film. The values for $\sqrt{t_{SD}}$ for the stretched and as-cast films and composites are listed in Table 3, along with the parameters used to calculate the domain sizes.

Converting the measured values for $\sqrt{t_{SD}}$ into domain sizes requires several parameters that may be estimated from the chemical structure or the relaxation times. The proton densities are estimated from the chemical structures and the density of Irogran, while the spin diffusion coefficients for mobile polymers are empirically related to the spin−spin relaxation times.[32] The spin diffusion coefficients for the rigid phase are assumed to be in the range of those reported for poly(styrene) and poly(methyl methacrylate) (0.8 nm^2/ms).[31] The volume fractions for the mobile and immobile phase are estimated from the chemical structure (Figure 1) and X-ray scattering data. The X-ray and DSC data show that the slightly stretched samples ($\lambda = 1.6$) have a crystallinity index of 1−3%. The immobile phase in these samples primarily results from self-association of the aromatic rings that are present at the 10% level. X-ray scattering shows a random structure at low draw ratios while a lamellar morphology with a crystallinity index of 40−50% is observed at high draw ratios ($\lambda = 11$).[25] Given these data, we have modeled the spin diffusion data using a three-dimensional spherical model at low draw ratios and a one-dimensional lamellar model at high draw ratios.

The results of the spin diffusion experiments listed in Table 3 show that the spin diffusion distance (L), the domain sizes (d), and spacings between domains (d_{lp}) depend strongly on the draw ratio but not on the presence of CNF's. At low draw ratios the domain sizes are on the order of 12−13 nm and the spacings between domains are in the range of 20−21 nm. High draw ratios lead to both smaller domain sizes (6−8 nm) and smaller spacings (12−14 nm). The domain spacings are in good agreement with those measured by X-ray scattering.[33]

Conclusion

The shape-memory thermoplastic polyurethane with 10% hard segments (Irogran) filled with CNF's have been studied using high-resolution solid-state proton NMR. Previous studies showed that Irogran has a complex morphology[9,25] and the incorporation of nanofibers further increased this complexity. The proton NMR signals from the mobile component in these films can be easily detected using high-resolution NMR methods because molecular motion in the mobile component averages the proton line widths from 50 kHz to 1−2 kHz. This allows us to monitor the polymer dynamics as CNF's are added and to measure the domain sizes using proton spin diffusion.

The addition of CNF's to Irogran leads to concentration-dependent changes in the chemical shifts and line widths of the mobile phase. The relaxation times are not sensitive to the

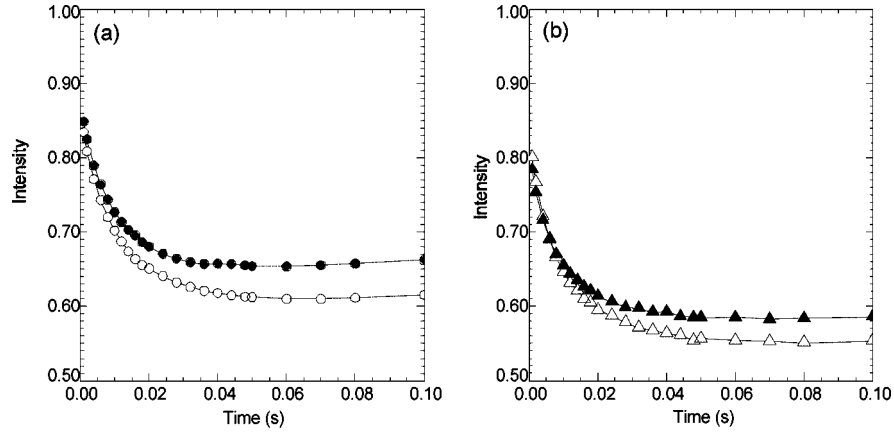

Figure 4. Magnetization exchange curves for as-cast (filled symbols) and stretched ($\lambda = 1.6$, open symbols) samples of (a) TPE films and (b) 10 wt % TPE/CNF composites.

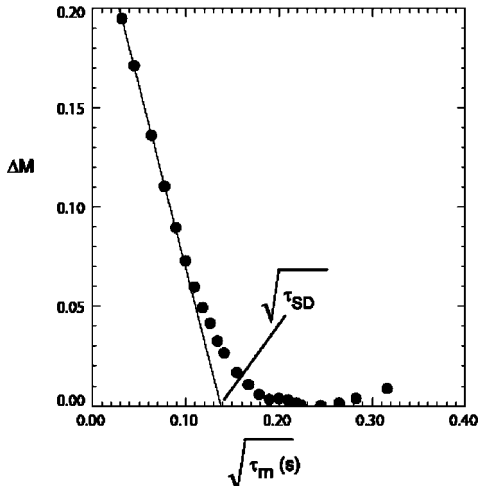

Figure 5. Spin diffusion plot for the as-cast TPE film sample.

Table 3. Spin Diffusion Times and Domain Sizes for Irogran Films and the 10 wt % CNF Composites[a]

sample	state	f[a]	D_{soft}[b] (nm²/ms)	$\sqrt{t_{SD}}$ (s$^{1/2}$)	L (nm)[c]	ε[d]	d (nm)[e]	d_{lp} (nm)[f]
Irogran	$\lambda = 1.0$	0.16	0.37	0.138	25.6	3	12	20
	$\lambda = 1.6$	0.16	0.31	0.147	26.7	3	12	21
	$\lambda = 11$	0.51	0.51	0.120	14.1	1	8	14
Irogran/10% CNF	$\lambda = 1.0$	0.19	0.40	0.136	23.6	3	13	20
	$\lambda = 1.6$	0.19	0.33	0.139	22.5	3	12	20
	$\lambda = 11$	0.51	0.43	0.110	11.9	1	6	11

[a] The hard segment fraction is the sum of the crystallinity determined by X-ray and the fraction of aromatic hard segments ($f = 0.1$). [b] D_a is the spin diffusion coefficient for the mobile amorphous phase determined from the spin−spin relaxation time. The diffusion coefficient for the rigid phase was taken as 0.8 nm²/ms. [c] The length scale of spin diffusion given by eq 3. [d] The dimensionality of the system. Spin diffusion was modeled as randomly distributed spheres ($\varepsilon = 3$) at low crystallinity where the hard segments are comprised mainly of self-associating hard segments. At high crystallinity X-ray studies show a lamellar morphology ($\varepsilon = 1$). [e] The domain sizes are given by $d = f_aL$ for $\varepsilon = 1$ and $d = 3f_aL$ for $\varepsilon = 3$. [f] The spacing between crystallites is given by $d_{lp} = L$ for $\varepsilon = 1$ and $d_{lp} = 2.683(f_a)^{2/3}L$ for $\varepsilon = 3$.

presence of CNF's, demonstrating that the broadening is inhomogeneous. We believe that the broadening and shifting is a consequence of the difference in magnetic susceptibility between the CNF's and the mobile polymer domains. This observation explains in part why it is difficult to directly observe the carbon spectra using cross polarization and magic-angle sample spinning in the presence of CNF's.

The stretching of Irogran and the 10 wt % CNF composites to 60% does not have a large effect on the molecular dynamics of the mobile domains or the crystallinity. We can observe differences in the spin diffusion curves at low draw ratios, suggesting that the NMR is extremely sensitive to the onset of stress-induced crystallization. Highly stretched samples ($\lambda = 11$) show significant differences in the chemical shifts, relaxation times, and domain sizes when compared to the slightly stretched samples. The similar chemical shifts for the highly drawn samples with and without CNF's suggest that the mobile phase is no longer in close proximity to the CNF's. These data support a model in which nucleation is promoted at the surface of the CNF's, thereby separating the mobile amorphous phase from the CNF's. Extreme stretching also increases the crystallinity and decreases the average domain sizes. The values for the spacing between domains measured by NMR are in good agreement with the values reported by X-ray scattering,[33] and they are in the same size range measured for other TPE's with low hard-segment fractions.[13]

In summary, we have used high-resolution solid-state proton NMR to probe the mobile amorphous phase in Irogran and its composites with CNF's. The results show that the signals are broadened in the vicinity of the CNF's due to a difference in magnetic susceptibility between the CNF's and the polymer, but the molecular dynamics are not greatly changed. Spin diffusion appears to be very sensitive to the onset of stress-induced crystallinity, and stretching to high draw ratios promotes crystallite formation on the surface of the CNF's and leads to a higher crystallinity and smaller crystallites.

Acknowledgment. We thank Professor Daniel Eylon from the Department of Chemical and Materials Engineering at the University of Dayton for guidance and support for D.S.P. during the course of this study.

References and Notes

(1) Lendlein, A.; Kelch, S. *Angew. Chem., Int. Ed.* **2002**, *41*, 2034–2057.
(2) Takahashi, T.; Hayashi, N.; Hayashi, S. *J. Appl. Polym. Sci.* **1996**, *60*, 1061–1069.
(3) Kim, B. K.; Lee, S. Y.; Xu, M. *Polymer* **1996**, *37*, 5781–5793.
(4) Phillips, L. N.; Parker, D. B. *Polyurethanes: Chemistry, Technology and Properties*; Iliffe Books Ltd.: London, 1964.
(5) Doyle, E. N. *The Development and Use of Polyurethane Products*; McGraw-Hill Inc.: New York, 1971.
(6) Curgul, S.; Yilgor, I.; Yilgor, E.; Erman, B.; Cakmak, M. *Macromolecules* **2004**, *37*, 8676–8685.
(7) David, D. J.; Staley, H. B. *Analytical Chemistry of the Polyurethanes*; Krieger Publishing Co.: Melbourne, FL, 1979; Vol. *16*.
(8) Smalley, R. E.; Dresselhaus, M. S.; Dresselhaus, G.; Avouris, P., Eds. *Carbon Nanotubes: Synthesis, Structure, Properties and Applications*; Springer: New York, 2001.

(9) Koerner, H.; Price, G.; Pearce, N.; Alexander, M.; Vaia, R. A. *Nat. Mater.* **2004**, *3*, 115–120.
(10) Brown, S. P.; Spiess, H. W. *Chem. Rev.* **2001**, *101*, 4125–4155.
(11) Assink, R. *Macromolecules* **1978**, *11*, 1233–1237.
(12) Demco, D. E.; Johansson, A.; Tegenfeldt, J. *Solid State NMR* **1995**, *4*, 13–38.
(13) Voda, M.; Demco, D. E.; Voda, A.; Schauber, T.; Alder, M.; Dabisch, T.; Adams, A.; Baias, M.; Blumich, B. *Macromolecules* **2006**, *39*, 4802–4810.
(14) Voda, A.; M, V.; Beck, K.; Schauber, T.; Alder, M.; Dabisch, T.; Bescher, M.; Viol, M.; Demco, D. E.; Blumich, B. *Polymer* **2006**, *47*, 2069–2079.
(15) Hou, S. S.; Beyer, F. L.; Schmidt-Rohr, C. *Solid State NMR* **2002**, *22*, 110–127.
(16) Kubies, D.; Jerome, R.; Grandjean, J. *Langmuir* **2002**, *18*, 6159–6163.
(17) VanderHart, D. L.; Asano, A.; Gilman, J. W. *Macromolecules* **2001**, *34*, 3819.
(18) Lin, W. Y.; Blum, F. D *J. Am. Chem. Soc.* **2001**, *123*, 2032–2037.
(19) Melosh, N. A.; Lipic, P.; Bates, F. S.; Wudl, F.; Stucky, G. D.; Fredrickson, G. H.; Chmelka, B. F. *Macromolecules* **1999**, *32*, 4332–4342.
(20) Marques, M. A. L.; d'Avezac, M.; Mauri, F. *Phys. Rev. B* **2006**, *73*, 125433–125436.
(21) Wang, C. S.; Alexander, M. *US Patent 6,680,016*, 2001.
(22) Mirau, P. *A Practical Guide to the NMR of Polymers*; John Wiley & Sons: Hoboken, NJ, 2004.
(23) Goldman, M.; Shen, L. *Phys. Rev.* **1966**, *144*, 321–331.
(24) Schmidt-Rohr, K.; Speiss, H. W. *Multidimensional Solid-State NMR and Polymers*; Academic Press: New York, 1994.
(25) Koerner, H.; Lui, W.; Alexander, M.; Mirau, P.; Dowty, H.; Vaia, R. A. *Polymer* **2005**, *46*, 4405–4420.
(26) English, A. D.; Debowski, C. *Macromolecules* **1984**, *17*, 446–449.
(27) Mirau, P. A.; Heffner, S.; Schilling, M. *Solid State NMR* **2000**, *16*, 47–53.
(28) Abragam, A. *Principles of Nuclear Magnetism*; Oxford University Press: New York, 1961.
(29) Blumler, P.; Blumich, B. *Acta Polym.* **1993**, *44*, 125.
(30) VanderHart, D. L.; McFadden, G. B. *Solid State NMR* **1996**, *7*, 45–66.
(31) Clauss, J.; Schmidt-Rohr, K.; Spiess, H. W. *Acta Polym.* **1993**, *44*, 1–17.
(32) Mellinger, F.; Wilhelm, M.; Spiess, H. *Macromolecules* **1999**, *32*, 4686–4691.
(33) Koerner, H.; Kelly, J.; Vaia, R. A. *Macromolecules* **2008**, *41*, in press.

MA8002483